

# An Arnoldi Approach for Generation of Reduced-Order Models for Turbomachinery

Karen Willcox and Jaime Peraire  
Department of Aeronautics and Astronautics

Jacob White  
Department of Electrical Engineering and Computer Science

Massachusetts Institute of Technology  
77 Massachusetts Avenue  
Cambridge, MA 02139

## Abstract

A linear reduced-order aerodynamic model is developed for aeroelastic analysis of turbomachines. The basis vectors are constructed using a block Arnoldi method. Although the model is cast in the time domain in state-space form, the spatial periodicity of the problem is exploited in the frequency domain to obtain these vectors efficiently. The frequency domain proper orthogonal decomposition is identified as a special case of the Arnoldi method. The aerodynamic model is coupled with a simple structural model that has two degrees of freedom for each blade. The technique is applicable to viscous and three-dimensional problems as well as multi-stage problems with inlet and exit disturbance flows, although here results are presented for two-dimensional, inviscid flow through a twenty-blade single-stage rotor. In this case, the number of states of the model is on the order of ten per blade passage, making it appropriate for control applications.

## 1 Introduction

With the current trend towards increased operating speeds and more flexible blading, aeroelasticity has become a critical consideration in the design of compressors. Understanding and predicting aeroelastic phenomena are crucial to ensuring that a compressor will operate within stability boundaries, and thus has a large impact on the design process. Appropriate blade design, together with strategies for controlling the onset of instabilities, can significantly impact the stable operating range, potentially leading to better compressor performance. In addition, understanding high cycle fatigue is important to prolong engine lifetimes.

Aeroelastic phenomena involve a complicated interaction between the aerodynamics and the structural dynamics of the blades. Typically, very simple aerodynamic models have been used for aeroelastic analyses of turbomachinery. The flow is usually assumed to be two-dimensional and potential [1]. These methods are useful near design conditions but inadequately predict the flow off-design, as blade loading effects become important [2]. The simple models are also inapplicable to transonic flows where shock dynamics play a significant role in determining the aerodynamic response. Transonic flow in a blade passage

can be determined by numerically solving the unsteady Euler or Navier-Stokes equations using computational fluid dynamics (CFD) methods, however such techniques are generally too computationally expensive to use for unsteady analyses, especially if the full rotor and more than one blade row need to be considered. More efficient methods for time-varying flow can be obtained if the disturbances are small, and the unsteady solution can be considered to be a small perturbation about a steady-state flow [3]. In this case, a set of linearised equations is obtained which can be time-marched to obtain the flow solution at each instant. However for control applications, any of the CFD based techniques will generate models with a prohibitively high number of states.

Reduced-order modelling for linear flow problems is now a well-developed technique and is reviewed in [4]. The basic idea is to project the high-fidelity CFD solutions onto a set of basis functions which span the flow solution space efficiently. Models are obtained which retain the high-fidelity aerodynamics of the CFD analysis, but which have only a few states. One possibility for a basis is to compute the eigenmodes of the system. This can lead to efficient models and the eigenmodes themselves often lend physical insight to the problem. However, typical problem sizes are on the order of tens of thousands of degrees of freedom per blade passage even in two dimensions, and solution of such a large eigen-problem is in itself a very difficult task. The proper orthogonal decomposition technique (POD) has been developed as an alternate method of deriving the basis functions [5] [6] and has been widely applied to many different problems. An efficient frequency domain use of the POD has been developed for solution of turbomachinery flows [7]. Since the basis vectors are obtained from solutions of the system, the reduced-order model produced by the POD is only applicable to flows very similar to those considered in the construction of the model. This raises an issue if the model is to be applied in a control framework, as we expect the dynamics of the controlled and uncontrolled systems to differ significantly [8].

In this paper an Arnoldi-based method is developed which provides an alternative to both the eigenmode and the POD approaches. The Arnoldi algorithm can be used to generate basis vectors which form an orthonormal basis for the Krylov subspace. The full set of Arnoldi vectors spans the same solution space as the system eigenvectors. An efficient reduced set can be constructed by considering both inputs and outputs of interest. Padé-based reduced-order models have been developed for linear circuit analysis using the Lanczos process [9]. This approach matches as many moments of the system transfer function as there are degrees of freedom in the reduced system. While the Arnoldi vectors match only half the number of moments as the Padé approximation, they preserve system definiteness and therefore often preserve stability [10].

Generation of reduced-order models from the two-dimensional linearised Euler equations will be considered here, however the approach could be easily extended to three-dimensional and viscous models if the underlying CFD model were available. The model will be developed in the time domain and cast in state-space form, and the resulting reduced-order model will have roughly ten states per blade passage. Simulation in the time domain allows for arbitrary forcing to be considered. It also enables the aerodynamics to be easily incorporated within a global engine model or coupled to an active control model. The small size of the reduced-order model makes it amenable to control design and mistuning analyses, and also allows for the full rotor to be considered and for the analysis of multi-stage problems.

In section 2 of this paper the underlying CFD model will be described. Some techniques for deriving reduced-order models will be discussed in section 3 and the reduction algorithm using the Arnoldi method will be presented and compared to the POD approach which is identified as a particular case of the Arnoldi method. Model reduction results will be presented in section 4 for a twenty-blade transonic rotor. The performance will be compared to both the linearised CFD simulation and the POD method. The aerodynamic reduced-order model will also be coupled to a simple two degree of freedom structural model for each blade and the coupled system behaviour investigated. Finally, in section 5 we present some conclusions.

## 2 Computational Model

### 2.1 Non-Linear Model

Consider an arbitrary two-dimensional time-varying control volume  $\Omega(t)$  with boundary  $\Gamma(t)$ . The Euler equations governing the unsteady, two-dimensional flow of an inviscid compressible fluid can be written in integral form as

$$\frac{\partial}{\partial t} \int_{\Omega} W dx dy + \oint_{\Gamma} (F n_x + G n_y) d\Gamma = 0, \quad (1)$$

where  $n_x$  and  $n_y$  are unit vectors pointing out of  $\Omega$ ,  $W$  is the unknown vector of conserved variables given by

$$W = (\rho, \rho u, \rho v, e)^T \quad (2)$$

and  $F$  and  $G$  are the inviscid flux vectors given by

$$F = \begin{pmatrix} \rho(u - x_t) \\ p + \rho u(u - x_t) \\ \rho v(u - x_t) \\ \rho u + e(u - x_t) \end{pmatrix}$$

$$G = \begin{pmatrix} \rho(v - y_t) \\ \rho u(v - y_t) \\ p + \rho v(v - y_t) \\ \rho v + e(v - y_t) \end{pmatrix}. \quad (3)$$

Here  $\rho$ ,  $u$ ,  $v$ ,  $p$  and  $e$  denote density, cartesian velocity components, pressure and total energy respectively.  $x_t$  and  $y_t$  are the speeds in the  $x$  and  $y$  directions with which the boundary  $\Gamma(t)$  moves. Also, for an ideal gas the equation of state becomes

$$e = \frac{p}{\gamma - 1} + \frac{1}{2} \rho (u^2 + v^2), \quad (4)$$

where  $\gamma$  is the ratio of specific heats.

To obtain a rectilinear two-dimensional representation of the cascade, the rotor is unwrapped in the circumferential direction as shown in figure 1. The boundaries extending upstream from the leading edge and downstream from the trailing edge of the blade surfaces

are periodic boundaries. To preserve the circumferential nature of the physical problem, a condition is enforced that the flow along the upper periodic boundary is the same as that along the lower periodic boundary. The governing equations are discretised using a finite volume formulation on an unstructured triangular grid covering this computational domain and approximations to the unknown flow vector  $W$  are sought at the vertices of that grid. For an interior vertex  $j$ , equation (1) can be written

$$\frac{d}{dt}(V_j W_j) + \int_{\Gamma_j} (F n_x + G n_y) d\Gamma = 0, \quad (5)$$

where  $V_j$  is the volume consisting of all the triangles having vertex  $j$ ,  $\Gamma_j$  is the boundary of  $V_j$  and  $W_j$  represents the average value of  $W$  over volume  $V_j$ . The integral in equation (5) is evaluated by considering weighted summations of flux differences across each edge in the control volume [11]. At boundary vertices, some of the flow variables are prescribed via appropriate boundary conditions. These prescribed quantities are contained within the vector  $\mathbf{U}_b$ , while the remaining unknown flow quantities are contained in the vector  $\mathbf{U}$ . For interior nodes the components of the unknown vector  $\mathbf{U}$  are the conservative flow variables (2), while for boundary nodes a coordinate transformation to other appropriate flow quantities is performed. The particular transformation depends on which flow quantities are to be specified via the boundary condition at that node.

Evaluation of (5) at each node combined with appropriate variable transformations leads to a large set of non-linear ordinary differential equations for the unknown flow vector  $\mathbf{U}$ , which can be written as

$$\frac{d\mathbf{U}}{dt} + R(\mathbf{U}, \mathbf{U}_b, \mathbf{x}) = 0, \quad (6)$$

where  $R(\mathbf{U}, \mathbf{U}_b, \mathbf{x})$  represents the non-linear flux contributions which are a function of the problem geometry  $\mathbf{x}$ , the flow solution  $\mathbf{U}$  and the boundary conditions  $\mathbf{U}_b$ .

We consider unsteady motion in which each blade can move with two degrees of freedom. For blade  $i$  the bending displacement (plunge) is denoted by  $h_i$  and torsion about an elastic axis (pitch) by  $\alpha_i$ . In general, blade shape deformations could also be included. The grid geometry  $\mathbf{x}$  depends directly on the positions of the individual blades, that is for  $r$  blades

$$\mathbf{x} = \mathbf{x}(h_1, \alpha_1, h_2, \alpha_2, \dots, h_r, \alpha_r). \quad (7)$$

At the passage inlet and exit we prescribe constant flow conditions, however flows with unsteady disturbances in the passages could be considered in an analogous way. For the specified quantities, we can therefore write

$$\mathbf{U}_b = \mathbf{U}_p(\mathbf{q}, \dot{\mathbf{q}}), \quad (8)$$

where  $\mathbf{q}$  is a vector containing the plunge and pitch displacements for each blade

$$\mathbf{q}_i = [h_i \ \alpha_i]^T, \quad (9)$$

and  $\mathbf{U}_p(\mathbf{q}, \dot{\mathbf{q}})$  contains the appropriate prescribed quantities.

## 2.2 Linearised Model

Steady-state solutions can be evaluated by driving the non-linear residual  $R(\mathbf{U}, \mathbf{U}_b, \mathbf{x})$  in (6) to zero, however to integrate the full non-linear equation in time for unsteady flows is computationally expensive, especially if the disturbances considered have circumferential variation. If we limit ourselves to the consideration of small amplitude unsteady motions, the problem can be considerably simplified by linearising the equations. We assume that the unsteady flow and grid geometry are small perturbations about a steady state

$$\begin{aligned}\mathbf{U}(\mathbf{x}, t) &= \bar{\mathbf{U}}(\mathbf{x}) + \mathbf{U}'(\mathbf{x}, t) \\ \mathbf{U}_b(\mathbf{x}, t) &= \bar{\mathbf{U}}_b(\mathbf{x}) + \mathbf{U}'_b(\mathbf{x}, t) \\ \mathbf{x}(t) &= \bar{\mathbf{x}} + \mathbf{x}'(t),\end{aligned}\tag{10}$$

and that the blade motions  $\mathbf{q}$  and  $\dot{\mathbf{q}}$  are small. Performing a Taylor expansion about steady-state conditions, for the unknown flow variables the non-linear residual in (6) can be written

$$R(\mathbf{U}, \mathbf{U}_b, \mathbf{x}) \simeq R(\bar{\mathbf{U}}, \bar{\mathbf{U}}_b, \bar{\mathbf{x}}) + \frac{\partial R}{\partial \mathbf{U}}(\bar{\mathbf{U}}, \bar{\mathbf{U}}_b, \bar{\mathbf{x}})\mathbf{U}' + \frac{\partial R}{\partial \mathbf{U}_b}(\bar{\mathbf{U}}, \bar{\mathbf{U}}_b, \bar{\mathbf{x}})\mathbf{U}'_b + \frac{\partial R}{\partial \mathbf{x}}(\bar{\mathbf{U}}, \bar{\mathbf{U}}_b, \bar{\mathbf{x}})\mathbf{x}'.\tag{11}$$

Using the fact that  $R(\bar{\mathbf{U}}, \bar{\mathbf{U}}_b, \bar{\mathbf{x}}) = 0$  and assuming that the perturbations are small so that quadratic and higher order terms in  $\mathbf{U}'$ ,  $\mathbf{U}'_b$  and  $\mathbf{x}'$  can be neglected, the linearised form of equation (6) is

$$\frac{d\mathbf{U}'}{dt} + \frac{\partial R}{\partial \mathbf{U}}\mathbf{U}' + \frac{\partial R}{\partial \mathbf{U}_b}\mathbf{U}'_b + \frac{\partial R}{\partial \mathbf{x}}\mathbf{x}' = 0,\tag{12}$$

where all derivatives are evaluated at steady-state conditions. Note that due to the linear assumption, the grid is not actually deformed for unsteady calculations, however the final term on the left-hand side of equation (12) represents the first order effects of grid motion. Likewise, the boundary conditions can be linearised to obtain

$$\mathbf{U}'_b = \frac{\partial \mathbf{U}_p}{\partial \mathbf{q}}\mathbf{q} + \frac{\partial \mathbf{U}_p}{\partial \dot{\mathbf{q}}}\dot{\mathbf{q}}.\tag{13}$$

We can further simplify the system by condensing  $\mathbf{U}'_b$  out of (12) using (13) and writing the grid displacement as a linear function of blade displacement

$$\mathbf{x}' = T\mathbf{q},\tag{14}$$

where  $T$  is a constant transformation matrix. The final set of ordinary differential equations then becomes

$$\frac{d\mathbf{U}'}{dt} + \frac{\partial R}{\partial \mathbf{U}}\mathbf{U}' = \left( -\frac{\partial R}{\partial \mathbf{x}}T - \frac{\partial R}{\partial \mathbf{U}_b}\frac{\partial \mathbf{U}_p}{\partial \mathbf{q}} \right)\mathbf{q} - \frac{\partial R}{\partial \mathbf{U}_b}\frac{\partial \mathbf{U}_p}{\partial \dot{\mathbf{q}}}\dot{\mathbf{q}},\tag{15}$$

which can be written equivalently as

$$\frac{d\mathbf{U}'}{dt} = A\mathbf{U}' + B\mathbf{u}.\tag{16}$$

Here  $\mathbf{u} = [\mathbf{q} \ \dot{\mathbf{q}}]^T$  is the input vector containing the displacement and velocity of each blade, and the matrix  $B$  contains the appropriate forcing terms of equation (15).

To determine the unsteady response of the cascade, the inputs  $\mathbf{u}(t)$  are specified and the large system (16) is time-marched to determine the resulting flow. Often we are not interested in obtaining the actual flow itself, but in relevant output quantities. These are typically the forces and moments acting on the blades, but could be any feature of the response. We define an output vector  $\mathbf{y}$  as

$$\mathbf{y} = C\mathbf{U}', \quad (17)$$

which for the analysis presented here contains the aerodynamic force and moment acting on each blade.  $C$  is a matrix containing the geometric contributions to the force calculation.

### 3 Reduction Using Congruence Transforms

The idea behind developing a reduced-order aerodynamic model is to project the large space used by a high-fidelity CFD model, such as that described in the previous section, onto a lower dimensional space which is characterised by a set of basis vectors. If these vectors are chosen so as to accurately span the solution space, the model behaviour can be captured with just a few states. In this way a low-order, high-fidelity aerodynamic model can be obtained. There are several options available for selecting the basis vectors, a few of which will be outlined here. It is desirable to choose an orthogonal set of vectors, as the resulting congruent transformation preserves the system definiteness, and therefore often preserves system stability.

If the set of  $q$  orthonormal basis vectors are contained in the columns of the matrix  $V_q$ , a  $q$ th order approximation to the perturbation solution can be made by assuming

$$\mathbf{U}' = V_q \mathbf{z}, \quad (18)$$

where  $\mathbf{z}(t)$  is the reduced-order aerodynamic state vector. Substituting this representation of  $\mathbf{U}'$  into the linearised governing equations (16) and premultiplying the system by  $V_q^T$ , we obtain the reduced-order system

$$\frac{d\mathbf{z}}{dt} = V_q^T A V_q \mathbf{z} + V_q^T B \mathbf{u}. \quad (19)$$

Writing the reduced-order matrices as  $A_r = V_q^T A V_q$  and  $B_r = V_q^T B$ , it is clear from (19) that the definiteness of the original system has been preserved. This can be seen by considering an arbitrary vector  $\mathbf{v}$ , then

$$\mathbf{v}^T A_r \mathbf{v} = \mathbf{v}^T V_q^T A V_q \mathbf{v} = (V_q \mathbf{v})^T A (V_q \mathbf{v}). \quad (20)$$

So the reduced system matrix  $A_r$  has the same definiteness as the original matrix  $A$ . A negative semidefinite matrix implies that all the eigenvalues have non-positive real part and the aerodynamic system is stable. In this case, if the original system is stable, so will be the reduced-order model. We note that this property is not preserved in transforms of the form  $A_r = W_q^T A V_q$  where  $W_q$  and  $V_q$  are bi-orthogonal.

### 3.1 Eigenmode Representation

An obvious choice might be to compute the eigenmodes of the large matrix  $A$  and to form the basis with the eigenvectors whose eigenvalues fall within the frequency range of interest. This approach has been taken for many problems, especially in structural dynamics where the matrices are generally symmetric and the eigenmodes are easy to compute. In fluid problems however, the eigenmodes of the very large matrix  $A$  are much more difficult to compute. Even in two dimensions it was found that for the full Euler equations the matrix was badly conditioned and that the eigenmodes suffered from non-normality problems. In addition, for a non-symmetric problem, both the right eigenvectors  $V_q$  and the left eigenvectors  $W_q$  must be computed, and the reduced matrix representation is of the form  $A_r = W_q^T A V_q$ . Although this is not a congruent transformation, a basis is obtained which preserves system stability, since the eigenvalues of the reduced-order model are a subset of the original system eigenvalues.

### 3.2 Proper Orthogonal Decomposition

The POD is a popular alternative to the eigenmode approach for determining a reduced-space basis. Typically, a time simulation of the system for a characteristic unsteady flow is performed and instantaneous solutions or snapshots are obtained at selected times. These snapshots are then combined to produce an orthogonal set of basis vectors which represents the solution  $\mathbf{U}'$  in some optimal way. More specifically, the basis vectors  $\Psi$  are chosen so as to maximise the following cost [5]:

$$\max_{\Phi} \frac{\langle |(\mathbf{U}', \Phi)|^2 \rangle}{(\Phi, \Phi)} = \frac{\langle |(\mathbf{U}', \Psi)|^2 \rangle}{(\Psi, \Psi)}, \quad (21)$$

where  $(\mathbf{U}', \Psi)$  denotes the scalar product of the basis vector with the field  $\mathbf{U}'(\mathbf{x}, t)$  and  $\langle \rangle$  represents a time-averaging operation.

A POD approach to developing reduced-order models for turbomachinery problems is presented in [7] and is summarised here. To avoid performing a time simulation of the large linearised system (16), the forcing is decomposed into spatial and temporal Fourier modes, and advantage is taken of the fact that the governing equations are linear to consider each of these modes separately. The temporal variation of the forcing can be viewed as a superposition of harmonic components each at a frequency  $\omega$ . This harmonic displacement of the  $N$  blades,  $\mathbf{u}$ , can then be thought of as comprising a superposition of  $N$  travelling wave modes [12]. This can be written for blade  $k$  as

$$u_k = \sum_{r=0}^{N-1} \bar{u}_r e^{i(\omega t + (k-1)\sigma_r)} \quad (22)$$

where the  $\bar{u}_r$  are complex coefficients. Here,  $\sigma_r$  is given by

$$\sigma_r = \frac{r2\pi}{N} \quad (23)$$

and is the interblade phase angle for the  $r$ th travelling wave. It describes the phase difference between the motion of a given blade and its neighbour [3]. Note that this does not mean we are restricted to consideration of sinusoidal motions, since by superposing these modes, any arbitrary disturbance in space and time may be represented.

Consider the component of blade motion at temporal frequency  $\omega_k$  and spatial frequency  $\sigma_j$ . The corresponding motion of the first blade can be written as

$$\mathbf{u}_1^{jk}(t) = \bar{\mathbf{u}}_1^{jk} e^{i\omega_k t}, \quad (24)$$

where  $\bar{\mathbf{u}}_1^{jk}$  contains the magnitudes of the blade position and velocity. The motion of any blade  $r$  can then be written in terms of the motion of the first blade as

$$\mathbf{u}_r^{jk}(t) = \bar{\mathbf{u}}_1^{jk} e^{i(r-1)\sigma_j} e^{i\omega_k t}. \quad (25)$$

The corresponding flow solution in each passage will also be harmonic of the form

$$\mathbf{U}_r^{jk}(t) = \bar{\mathbf{U}}_1^{jk} e^{i(r-1)\sigma_j} e^{i\omega_k t}, \quad (26)$$

with the same spatial frequency  $\sigma_j$  because all blades have the same aerodynamic shape and so the  $j$ th spatial forcing only excites the  $j$ th spatial aerodynamic response. Here the vector  $\mathbf{U}_r$  represents the unknown perturbation flow variables associated with blade  $r$ . In addition, since each  $\bar{\mathbf{U}}_1^{jk}$  contains a single spatial frequency, if the response of the first blade is known, then the response of all subsequent blades can be determined by using (26). The governing equations can therefore be discretised on a single blade passage making the computation much more efficient than a time domain calculation. The linearised Euler equations (16) can now be cast in the frequency domain on a single passage as

$$[i\omega_k - A_j] \bar{\mathbf{U}}_1^{jk} = B \bar{\mathbf{u}}_1^{jk}, \quad (27)$$

where  $A_j$  represents the original matrix  $A$  for just one passage, but modified to allow for a complex periodicity condition. This condition enforces the fact that the flow along the upper periodic boundary is the same as that along the lower periodic boundary but shifted in phase by the interblade phase angle  $\sigma_j$ .

Resulting solutions of the frequency domain CFD equations (27) provide an image of the flow at each temporal frequency  $\omega_k$ , for each spatial frequency  $\sigma_j$ . The real and imaginary parts of this image form the snapshots for the POD analysis. Although far more efficient than a POD analysis in the time domain, this approach requires the factorisation of the matrix  $[i\omega_k - A_j]$  for each pair of frequencies. For a typical bladed disk, the cost of generating the snapshots can be high if a large frequency range is to be considered. Another issue with the POD approach is that it is necessary to arbitrarily specify a set of sample frequencies. Typically some knowledge will be available on the range of frequencies expected to be present in the system response, and the POD will be sampled over this range. However it is also necessary to choose exactly which frequencies will be sampled within this range. If samples are placed too far apart, important system dynamics may be missed; if they are placed too closely together, a large number of matrix factorisations and solves is necessary and so the cost of generating the model becomes high.



### 3.3 Arnoldi-Based Model Order Reduction

An approach which can be thought of as a compromise between the eigenmode and POD methods is developed in this section. While the basis is easy to compute, some of the issues associated with the sampling requirements in the POD are addressed. Our basic goal is to obtain a reduced system which has many fewer states than the original system, can be computed with a reasonable cost, but which still represents the original system's dynamics accurately. One approach to ensuring accurate representation of system dynamics is to try to match the transfer functions of the reduced and the original systems. Consider first a single input, single output system

$$\dot{\mathbf{U}}' = A\mathbf{U}' + \mathbf{b}u, \quad y = \mathbf{c}^T \mathbf{U}'. \quad (28)$$

The transfer function between input  $u(t)$  and output  $y(t)$  is

$$H(s) = \mathbf{c}^T (sI - A)^{-1} \mathbf{b}, \quad (29)$$

which can also be represented as a rational function

$$H(s) = \frac{N(s)}{D(s)}, \quad (30)$$

where the numerator  $N(s)$  and denominator  $D(s)$  are both polynomials in  $s$ . A  $q$ th order Padé approximation to the transfer function is defined as

$$H_q(s) = \frac{b_{q-1}s^{q-1} + \dots + b_1s + b_0}{a_qs^q + a_{q-1}s^{q-1} + \dots + a_1s + 1}. \quad (31)$$

The  $2q$  coefficients of the Padé approximation,  $a_j$ ,  $b_j$ , can be selected so as to match the first  $2q$  terms in a McLaurin expansion of the transfer function (29). We can write

$$H(s) = - \sum_{k=1}^{\infty} m_k s^k, \quad (32)$$

where

$$m_k = \mathbf{c}^T A^{-(k+1)} \mathbf{b} \quad (33)$$

is the  $k$ th moment of  $H(s)$ . A  $q$ th order Padé approximation can be constructed via the Lanczos process and will match the first  $2q$  moments of  $H(s)$  [9].

An alternative approach is to use the Arnoldi method to generate a set of vectors which spans the  $q$ th order Krylov subspace defined by

$$\mathcal{K}_q(A, \mathbf{b}) = \text{span}\{A^{-1}\mathbf{b}, A^{-2}\mathbf{b}, \dots, A^{-q}\mathbf{b}\}. \quad (34)$$

The set of  $q$  Arnoldi vectors matches  $q$  moments of the system transfer function, that is half the number matched by the Padé approximation, however since the Arnoldi approach has the advantage of generating a congruent transformation, in many cases it generates models

with guaranteed stability. It is possible to reduce systems with multiple inputs using the block Arnoldi method. For example, if we consider a system with two inputs  $u_1$  and  $u_2$ ,

$$\dot{\mathbf{U}}' = A\mathbf{U}' + \mathbf{b}_1u_1 + \mathbf{b}_2u_2, \quad (35)$$

then the block Arnoldi method is used to generate vectors which span the Krylov subspace

$$\mathcal{K}_q(A, \mathbf{b}_1, \mathbf{b}_2) = \text{span}\{A^{-1}\mathbf{b}_1, A^{-1}\mathbf{b}_2, A^{-2}\mathbf{b}_1, A^{-2}\mathbf{b}_2, \dots, A^{-q}\mathbf{b}_1, A^{-q}\mathbf{b}_2, \}. \quad (36)$$

We also note that it is not necessarily the first  $q$  moments which must be matched. If we were to consider a Taylor series expansion of the transfer function about some non-zero value of  $s$ , a model could be obtained which would give a better approximation of the system dynamics for higher frequencies. These multiple frequency point Arnoldi methods are described in [13].

In order to calculate the basis, we consider input vectors which correspond to a particular blade having a unit displacement or velocity and all other blades fixed. Although vectors must be constructed for each of the  $N$  blades being perturbed in turn, the calculation need only be performed once, with the remaining  $N - 1$  vectors constructed through symmetry considerations. Once again, we can use linearity to decompose this forcing into a set of orthogonal modes each containing a single spatial frequency, and the calculation for each of these modes can be performed on a single blade passage. For expansions of the transfer function about  $s = i\omega_k$ , solutions of the complex frequency domain equations (27) must be obtained. The resulting solutions are then combined via an inverse Fourier transform to obtain the first blade basis vector. Vectors for subsequent blades are computed through use of symmetry. Further simplification can be obtained by noting that for expansions about  $s = 0$ , the set of Arnoldi vectors for spatial frequencies  $\sigma$  and  $-\sigma$  are complex conjugates of one another. The algorithm for the single input, single output case expanded about  $\omega_k$  is shown below.

**Algorithm 3.1 (Arnoldi Method)**

```

arnoldi(input  $A, \mathbf{b}, \omega_k, q_k, N$ ; output  $V_q$ )
{
  for ( $j = 1; j \leq N; j++$ ) {
    Factor  $[i\omega_k - A_j]$ 
    Solve  $[i\omega_k - A_j]\mathbf{v}_1 = \mathbf{b}$ 
    for ( $k = 1; k \leq q_k; k++$ ) {
      Solve  $[i\omega_k - A_j]\mathbf{w} = \mathbf{v}_k$ 
      for ( $i = 1; i \leq k; i++$ ) {
         $h = \mathbf{w}^T \mathbf{v}_i$ 
         $\mathbf{w} = \mathbf{w} - h\mathbf{v}_i$ 
      }
       $\mathbf{v}_{k+1} = \frac{\mathbf{w}}{\|\mathbf{w}\|}$ 
    }
     $V_q^j = [\mathbf{v}_1 \dots \mathbf{v}_q]$ 
  }
}

```

Given the set of basis vectors  $V_q$ , we substitute the projection of  $\mathbf{U}'$  (18) into the governing equations (16) and (17) to obtain the reduced-order system (19) which can be written as

$$\frac{d\mathbf{z}}{dt} = A_r \mathbf{z} + B_r \mathbf{u}, \quad \mathbf{y} = C_r \mathbf{z}. \quad (37)$$

One can see the similarities between the POD approach and the multiple frequency point Arnoldi method. In fact, solving the system (27) at  $J$  frequencies to obtain the POD snapshots results in an identical data set as taking  $J$  frequency points and computing a single Arnoldi vector at each point (the subsequent orthogonalisation procedure differs between the two methods). Very efficient models could be constructed by considering a range of frequencies and using the POD analysis to choose the basis vectors, but also computing more than one vector at each frequency as in the Arnoldi approach. One must evaluate the relative gain in choosing a higher number of frequency points, since by far the most expensive part of the calculation is the factorisation of the matrix in solving the linear system. In the Arnoldi approach, the matrix is computed and factored just once for each  $\omega_k$  and  $\sigma_j$ , but as outlined in the Algorithm 3.1,  $q_k$  vectors are obtained per factorisation. As mentioned previously, for the POD a different matrix must be factored for every solve.

## 4 Results

### 4.1 Aerodynamic Reduced-Order Model for Transonic Cascade

Reduced-order models have been developed for subsonic and transonic cascades operating with general unsteady blade motion. A DFVLR L030-4 transonic rotor which operates at a steady-state inlet Mach number of 0.82 was analysed in unsteady plunging motion for a twenty-blade configuration. Figure 2 shows the grid for two passages of this rotor. The steady-state solution is shown in figure 3.

Arnoldi basis vectors were computed for the interblade phase angles present in the twenty-blade configuration. For plunging motion there are two inputs per blade - the plunge position  $h$  and the plunge velocity  $\dot{h}$ . The reduced-order aerodynamic model was constructed and the eigenvalue spectrum of this system is shown in figure 4. For the case shown, there are six states for the zero interblade phase angle case and ten states for all other interblade phase angles (twenty for each pair  $\sigma, -\sigma$ ), giving a total of 196 states in the reduced-order model. Note that  $\sigma = 0$  is a special case where the plunge position  $h$  has no effect, and less modes are required to accurately capture the dynamics. Comparatively, the CFD computational grid for twenty passages would have 71940 grid points, which corresponds to 287760 unknowns. Clearly a time-domain computation of this size is very expensive, however we will show that the cascade dynamics can be accurately captured with the above choice of less than two hundred states in the reduced-order model.

Forced response of the cascade to a pulse input is a good assessment of the model's capability, since a pulse contains a continuous spectrum of temporal frequencies. Comparison of reduced-order modelling predictions with results from the full simulation code (if these results were available) would determine how many modes are required to accurately capture

the system dynamics. The input takes the form

$$h(t) = he^{-g(t-t_0)^2}, \quad (38)$$

where  $g$  is a parameter which determines how sharp the pulse is and thus the value of the highest significant frequency present.

As mentioned, it would be very expensive to perform a time simulation of the linearised CFD code on the full rotor. However if all blades are supplied with the same pulse input, a motion results in which only an interblade phase angle of zero is present and which can be solved using the linearised simulation code with just a single passage. The corresponding blade position input and non-dimensional vertical component of force response on each blade as a function of time are depicted in figures 5 and 6. It shows that excellent agreement is obtained with only a handful of states in the reduced-order model. This same case was considered using a reduced-order model constructed with the POD technique described in [7]. The POD samples were made at ten equally spaced reduced frequencies over the range  $k = 0 - 1.22$  for each interblade phase angle. This frequency range spans the important content of the pulse for a value of  $g = 0.01$ . The response calculated with the POD reduced-order model is also shown in figure 6. Although the POD response is more accurate than the Arnoldi response with four modes, with six modes the Arnoldi model is very close to the linearised simulation response, while the POD slightly underpredicts the force at both peaks.

For this problem, a total of two hundred matrix factorisations were performed to obtain the POD snapshots (ten sample frequencies for each of twenty interblade phase angles). In comparison, just eleven matrix factorisations were required for the Arnoldi reduced-order model since all vectors were computed about  $s = 0$ . The Arnoldi-based model is an order of magnitude cheaper to obtain than the POD model, and also does a better job of predicting the response. In addition, the POD reduced-order model is restricted to responses containing frequencies within the (arbitrary) sample range. The Arnoldi-based model contains no such restriction, although more modes will be required if flows containing higher frequencies are to be modelled. In this case, one might choose to use a multiple frequency point method as described earlier. The reduced-order models obtained using the POD method are very sensitive to the choice of sample frequencies. As mentioned previously, it is necessary to ensure not only that the correct range is sampled, but also that enough samples are performed over this range, or the system dynamics will not be accurately captured. Because more than one vector is computed at each frequency in the Arnoldi method, the dynamics can be captured without considering many frequency points (one can liken the Arnoldi approach to computing higher-order “derivatives” at each frequency point). An appropriate choice of frequency points can reduce the required size of the reduced-order models, but is not necessarily required to capture system dynamics, as the example presented here demonstrates.

The reduced-order model was also used to calculate forced response of the twenty-blade cascade to sinusoidal motion at an interblade phase angle of  $90^\circ$ . The linearised CFD solution can be obtained for this flow using just a single passage in the frequency domain. The calculated force on the first blade is shown as a function of time in figure 7. The results for the reduced-order model with twelve, sixteen and twenty states for this interblade phase

angle are compared to those obtained from the CFD frequency domain code. The results obtained with twenty modes in the reduced-order model are virtually indistinguishable from the CFD. The required size of the Arnoldi reduced-order model for this case is a little larger than that found to be necessary for the POD approach, which typically used around twelve modes for a purely sinusoidal motion. However, the POD snapshots were generated using sinusoidal motions, so we expect them to predict such a response very efficiently. As seen with the pulse response described above, the Arnoldi approach does a much better job with general inputs as there is no assumed relation between position and velocity when forming the modes.

A case was then considered where just one blade was forced with the pulse input, while all others were held fixed. This motion contains all possible interblade phase angles. The response for each blade was computed using the Arnoldi reduced-order model with 196 aerodynamic states. The inputs and response of each blade are shown in figure 8. This computation was far too expensive to be carried out with the linearised simulation code. It is clear from the plot that the largest force is generated on the disturbed blade and its nearest neighbours, as might be expected intuitively. We can see that beyond the two closest blades the force generated is very small.

## 4.2 Structural Coupling

For analysis of forced response, the blade motion inputs  $\mathbf{u}_j$  are specified and the system (37) is time-marched to determine the resulting aerodynamic response. For a coupled analysis, equations of motion describing the structural states must be included in the reduced-order model. We might be interested in investigating the stability of the coupled system, or in determining the overall response to a perturbation in blade position. The structural model could be a complicated system (for example a reduced-order structural model derived from a finite element analysis) or a simple model (for example a very low-order mass-spring model). We consider here a simple mass-spring-damper structural model where each blade can move in plunging motion with a natural frequency of  $\omega_h$  as shown in figure 9. For plunge only, the structural equations of motion for each blade with mass  $m$  and chord  $c$  can be written as

$$\frac{d}{dt} \begin{bmatrix} h_j \\ \dot{h}_j \end{bmatrix} = \begin{bmatrix} 0 & 1 \\ -(kM)^2 & -2kM\zeta \end{bmatrix} \begin{bmatrix} h_j \\ \dot{h}_j \end{bmatrix} + \begin{bmatrix} 0 \\ \frac{2M^2}{\pi\mu} \end{bmatrix} C_l^j, \quad (39)$$

or in matrix form,

$$\dot{\mathbf{u}} = S\mathbf{u} + T\mathbf{y}. \quad (40)$$

In the above, the reduced frequency is defined in terms of the plunge natural frequency  $k = \frac{\omega_h c}{V}$ ,  $\zeta$  is the structural damping coefficient and  $\mu = \frac{4m_i}{\pi \rho c^2}$  is the blade mass ratio.  $C_l^j = y_j$  is the lift coefficient for blade  $j$ , and  $M$  and  $V$  are the inlet Mach number and axial velocity respectively. This structural model is then coupled to the aerodynamic reduced-order state-space system (37). The coupled system is as follows :

$$\begin{bmatrix} \dot{\mathbf{z}} \\ \dot{\mathbf{u}} \end{bmatrix} = \begin{bmatrix} A_r & B_r \\ TC_r & S \end{bmatrix} \begin{bmatrix} \mathbf{z} \\ \mathbf{u} \end{bmatrix}. \quad (41)$$

At each timestep the structural and aerodynamic equations are thus solved simultaneously to determine the blade position and velocity and the aerodynamic forces acting.

The eigenvalues of the tuned coupled system (41) for a reduced frequency of  $k = 0.25$ , no structural damping and a mass ratio of  $\mu = 100$  are shown in 10. We observe some movement of the original aerodynamic eigenvalues due to interaction with the structure, and also the introduction of forty structural modes with frequencies around the natural frequency  $kM = 0.205$ . A zoom of these structural eigenvalues is shown in figure 11.

A time-marching simulation of the coupled system was run with  $k = 0.25$  and  $\zeta = 0$ . An initial plunge displacement was applied to one of the blades, then the coupled structural and aerodynamic response for the entire rotor was computed. Figure 12 shows the resulting displacement and lift force for each blade. Clearly the disturbed blade (blade 3) exhibits the largest response. The resulting motion is decaying, although slowly since the coupled system is lightly damped.

## 5 Conclusions

A new method of producing reduced-order models for turbomachinery has been demonstrated. This method provides an excellent alternative to the eigenmode and POD approaches to reduced-order modelling. The basis vectors are constructed efficiently by applying the Arnoldi method to the frequency domain governing equations, while development of the model in the time domain allows for ease of coupling to actuation and control models and provides a convenient framework for integration within more global engine models. The framework developed is particularly suited to the analysis of mistuned rotors where the interblade phase angles do not decouple and the entire rotor must be considered. It is also straightforward to extend this approach to viscous and three-dimensional flows if the underlying CFD model is available.

The Arnoldi basis has the benefits of an eigenmode approach in that it models the dynamics of the original high-order system, but it is much more straightforward to compute. The Arnoldi-based models are much cheaper to compute than those constructed using the POD since one matrix factorisation can be used to obtain many basis vectors, and are in general applicable to a wider range of flows. It is also possible to use Arnoldi methods with multiple frequency points to obtain efficient models which are valid for flows containing higher frequencies, however the models obtained are less sensitive than POD-based models to the choice of sample frequencies. In addition, outputs of interest can be included in the criterion for selecting the basis vectors, and further improvement can be obtained by post-processing the resulting reduced-order models using a truncated balanced realisation.

## Acknowledgments

The authors wish to acknowledge helpful discussions with Dr. James Paduano. Support for this work has been provided by the AFOSR PRET program. J. Paire and J. White also acknowledge the support of the Singapore MIT Alliance and the DARPA MURI program.

## References

- [1] D.S. Whitehead. Classical Two-Dimensional Methods. AGARD Manual on Aeroelasticity in Axial-Flow Turbomachines, Unsteady Turbomachinery Aerodynamics, Volume 1, 1987.
- [2] J.M. Verdon. Review of Unsteady Aerodynamic Methods for Turbomachinery Aeroelastic and Aeroacoustic Applications. *AIAA Journal*, 31(2):235–250, February 1993.
- [3] K.C. Hall. *A Linearized Euler Analysis of Unsteady Flows in Turbomachinery*. PhD thesis, Dept. of Aeronautics and Astronautics, MIT, May 1987.
- [4] E.H. Dowell, K.C. Hall, J.P. Thomas, R. Florea, B.I. Epureanu, and J. Heeg. Reduced Order Models in Unsteady Aerodynamics. AIAA 99-1261, 1999.
- [5] L. Sirovich. Turbulence and the Dynamics of Coherent Structures. Part 1 : Coherent Structures. *Quarterly of Applied Mathematics*, 45(3):561–571, October 1987.
- [6] G. Berkooz, P. Holmes, and J.L. Lumley. The Proper Orthogonal Decomposition in the Analysis of Turbulent Flows. *Annual Review of Fluid Mechanics*, 25:539–575, 1993.
- [7] K.E. Willcox, J.D. Paduano, J. Peraire, and K.C. Hall. Low Order Aerodynamic Models for Aeroelastic Control of Turbomachines. AIAA 99-1467, 1999.
- [8] K.Y. Tang, W.R. Graham, and J. Peraire. Active Flow Control Using a Reduced Order Model and Optimum Control. AIAA 96-1946, 1996.
- [9] P. Feldmann and R.W. Freund. Efficient Linear Circuit Analysis by Padé Approximation via the Lanczos Process. *IEEE Transactions on Computer-Aided Design of Integrated Circuits and Systems*, 14:639–649, 1995.
- [10] L.M. Silveira, M. Kamon, I. Elfadel, and J. White. A Coordinate-Transformed Arnoldi Algorithm for Generating Guaranteed Stable Reduced-Order Models of RLC Circuits. *Computer Methods in Applied Mechanics and Engineering*, 169(3-4):377–389, February 1999.
- [11] Karen E. Willcox. Aeroelastic Computations in the Time Domain Using Unstructured Meshes. Master’s thesis, Dept. of Aeronautics and Astronautics, MIT, February 1996.
- [12] J. Dugundji and D.J. Bundas. Flutter and Forced Response of Mistuned Rotors Using Standing Wave Analysis. *AIAA Journal*, 22(11):1652–1661, November 1984.
- [13] E. Grimme. *Krylov Projection Methods for Model Reduction*. PhD thesis, Coordinated-Science Laboratory, University of Illinois at Urbana-Champaign, 1997.

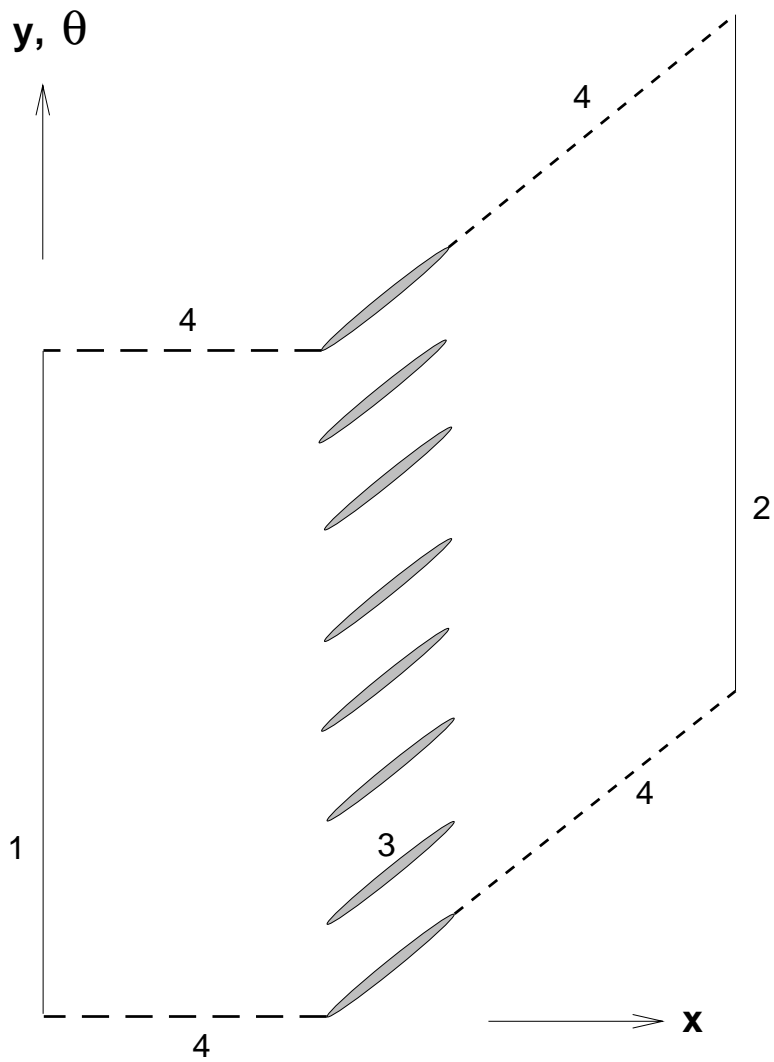


Figure 1: Rectilinear two-dimensional representation of cascade. Inlet boundary (1), exit boundary (2), blade surfaces (3) and periodic boundaries (4).



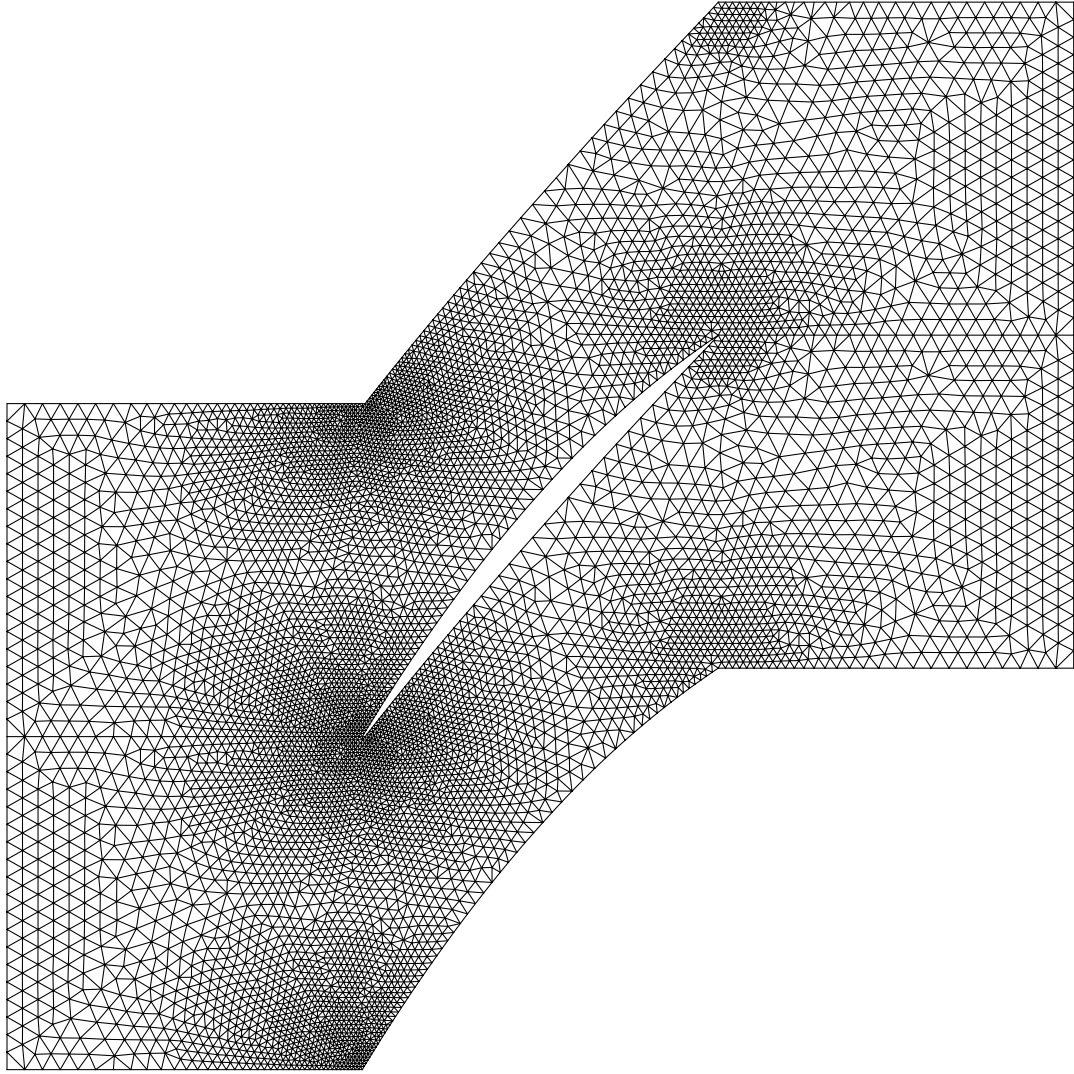


Figure 2: Computational domain for two blade passages, DFVLR transonic rotor. 3597 nodes, 7040 triangles per blade passage.

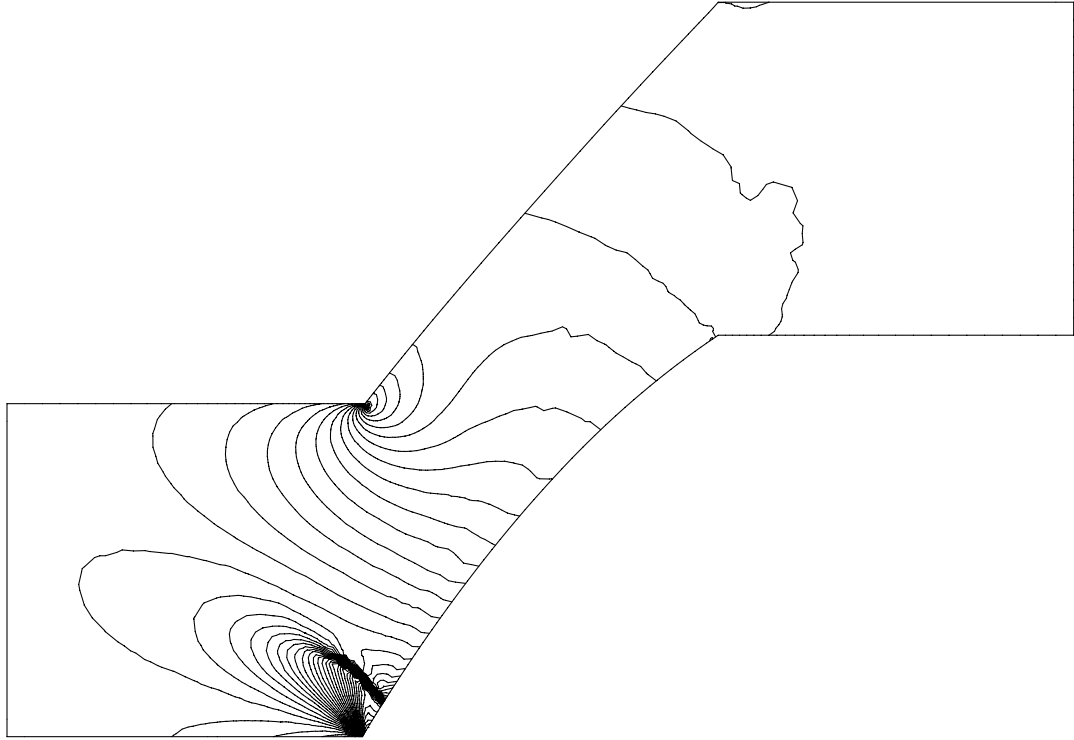


Figure 3: Pressure contours for steady inviscid transonic flow.  $M = 0.82$ ,  $\alpha = 58.5^\circ$ .

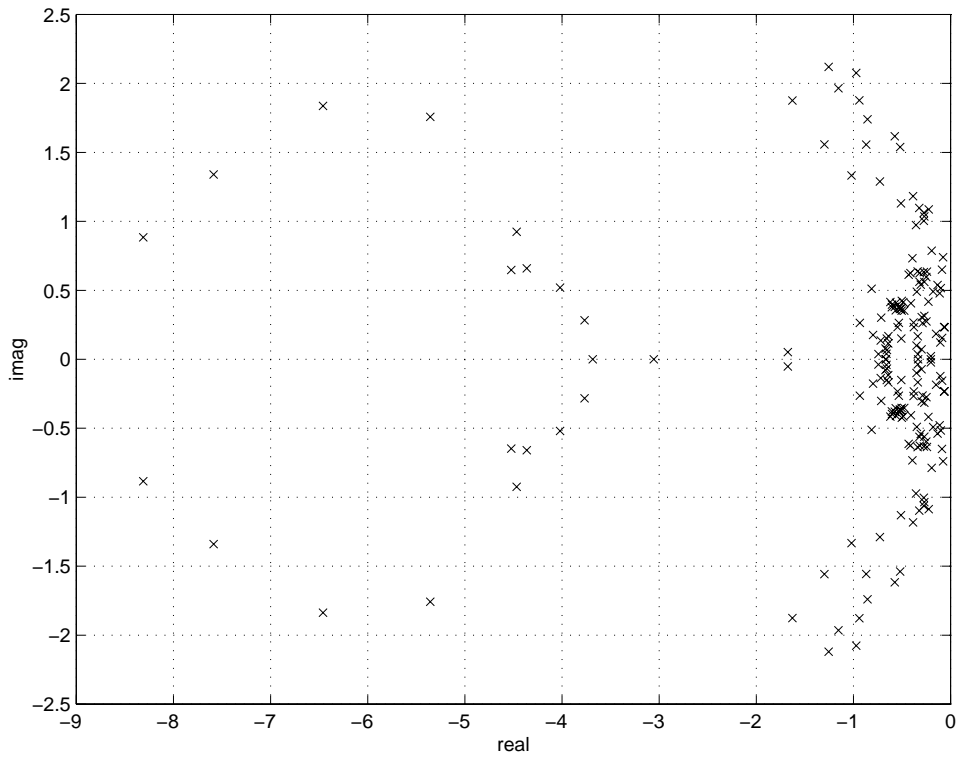


Figure 4: Eigenvalue spectrum for Arnoldi reduced-order aerodynamic system. 6 states for  $\sigma = 0^\circ$ , 10 states for all other  $\sigma$  (total 196 states).

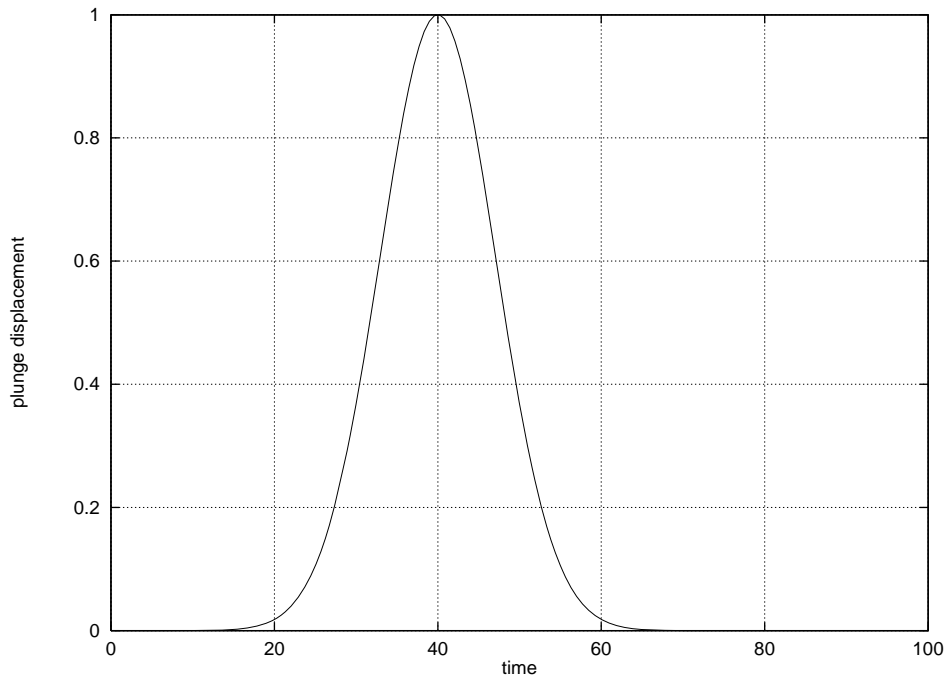


Figure 5: Pulse input in plunge.

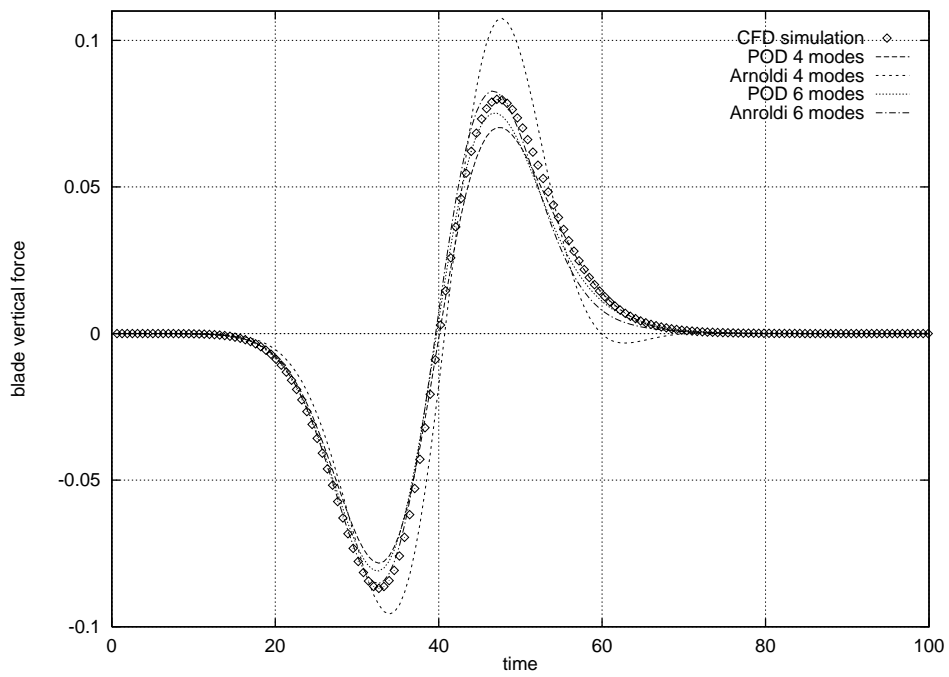


Figure 6: Pulse response for Arnoldi and POD reduced-order models and linearised simulation code.  $\sigma = 0^\circ$ ,  $g = 0.01$ ,  $M = 0.82$ .

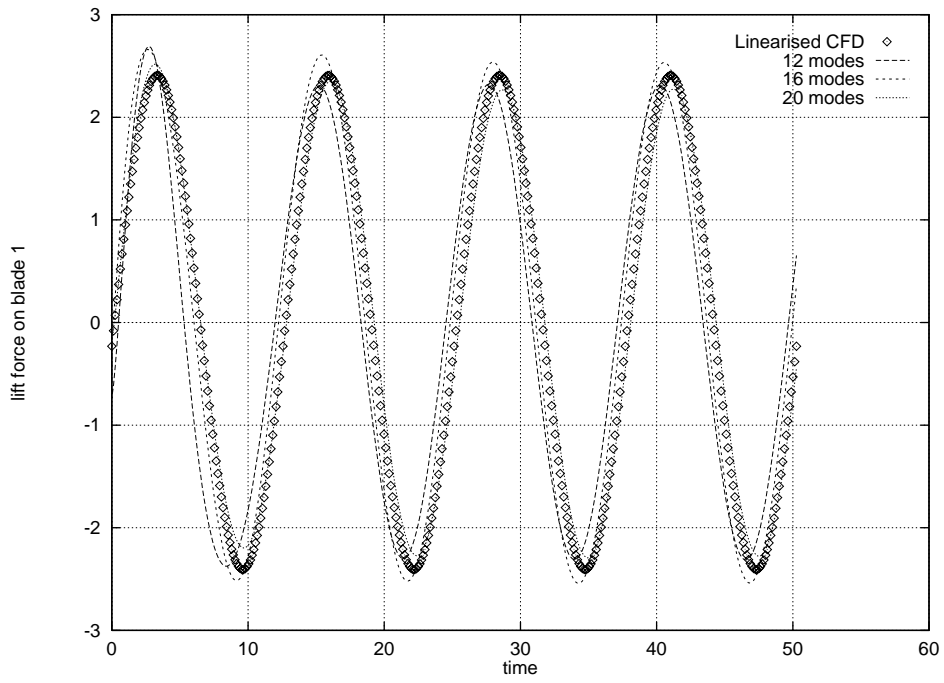


Figure 7: Forced response of first blade to sinusoidal motion using Arnoldi reduced-order model and CFD frequency domain code.  $\sigma = 90^\circ$ ,  $\omega = 0.5$ ,  $M = 0.82$ .

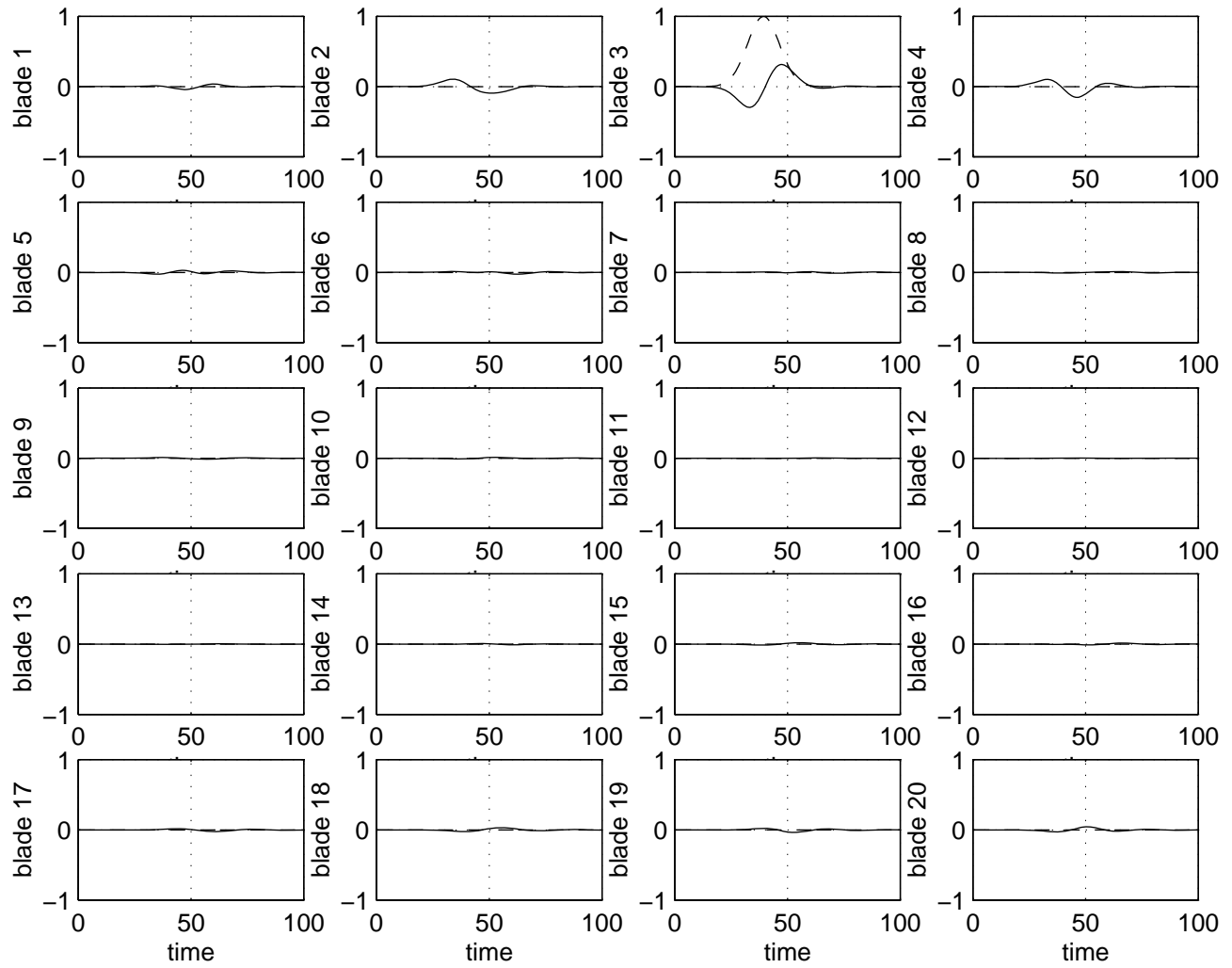


Figure 8: Pulse displacement input at blade 3 (dashed line) and blade lift force response (solid line) for Arnaldi reduced-order model. 196 aerodynamic states,  $g = 0.01$ ,  $M = 0.82$

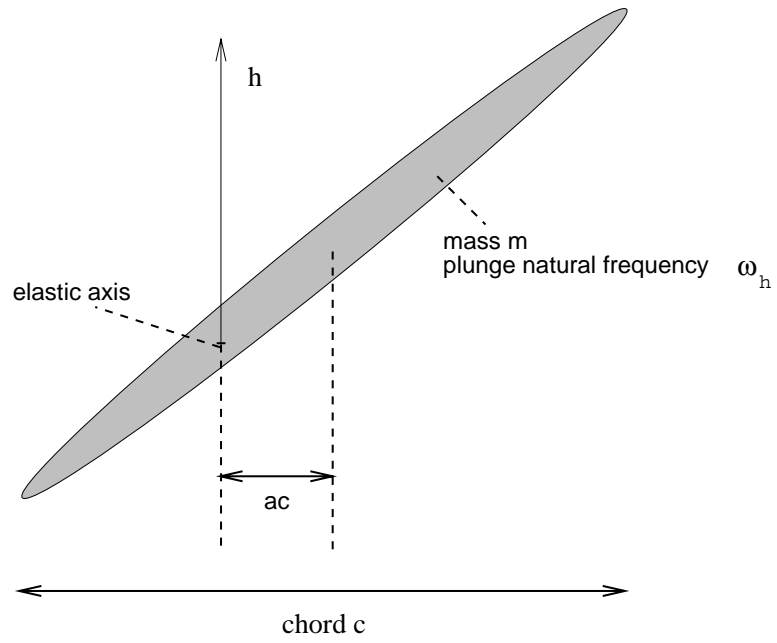


Figure 9: Typical section structural model for plunging motion of blade  $i$ .

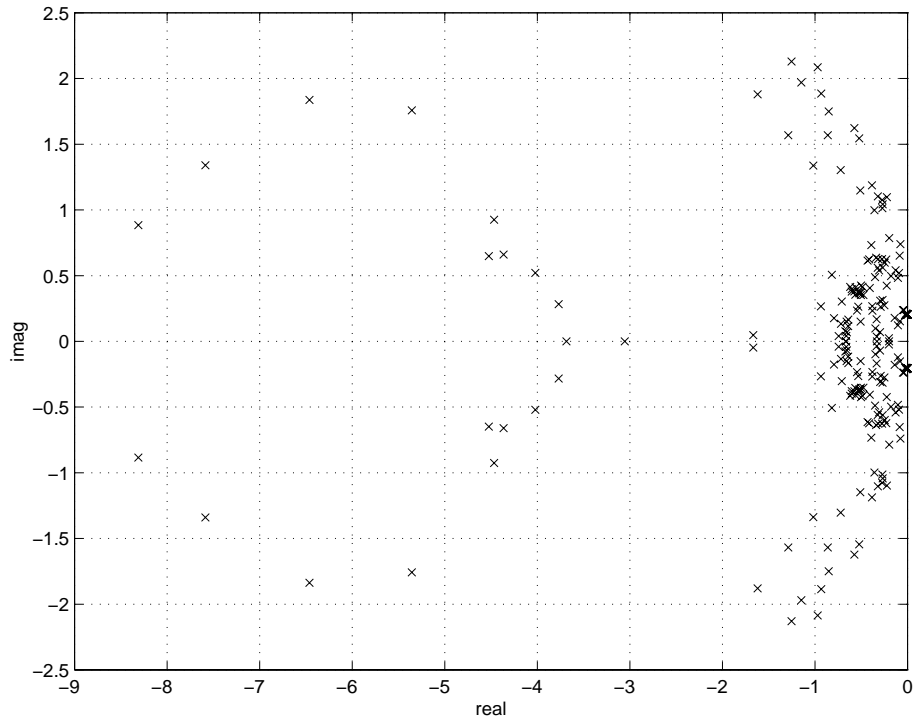


Figure 10: Eigenvalue spectrum for coupled system. 196 aerodynamic states, 40 structural states.  $M = 0.82$ ,  $\mu = 100$ ,  $k = 0.25$ ,  $\zeta = 0$ .

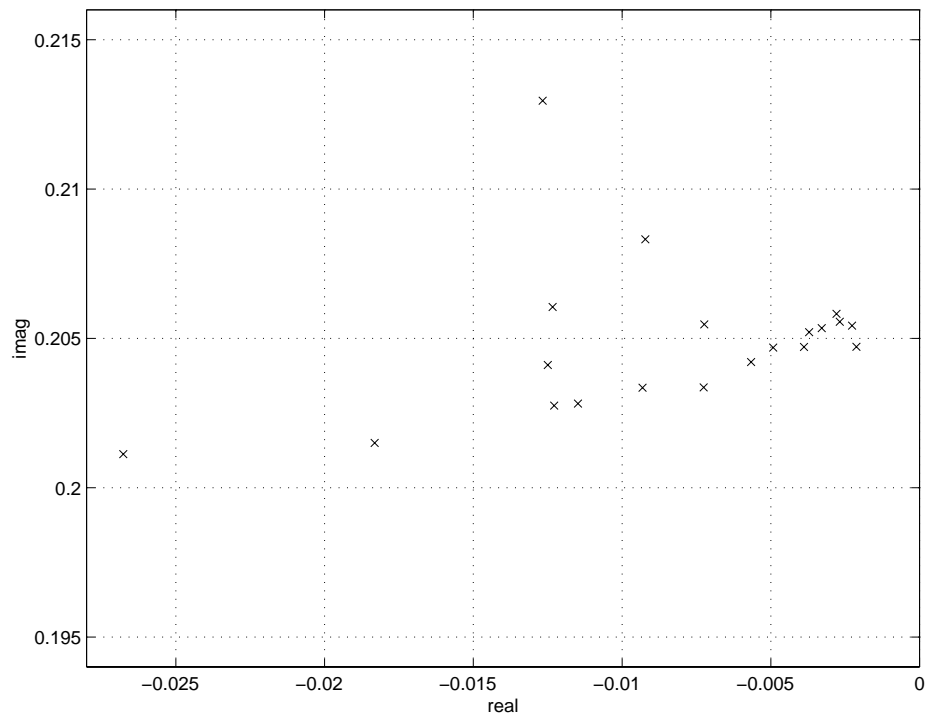


Figure 11: Zoom of structural eigenvalues.  $M = 0.82$ ,  $\mu = 100$ ,  $k = 0.25$ ,  $\zeta = 0$ .

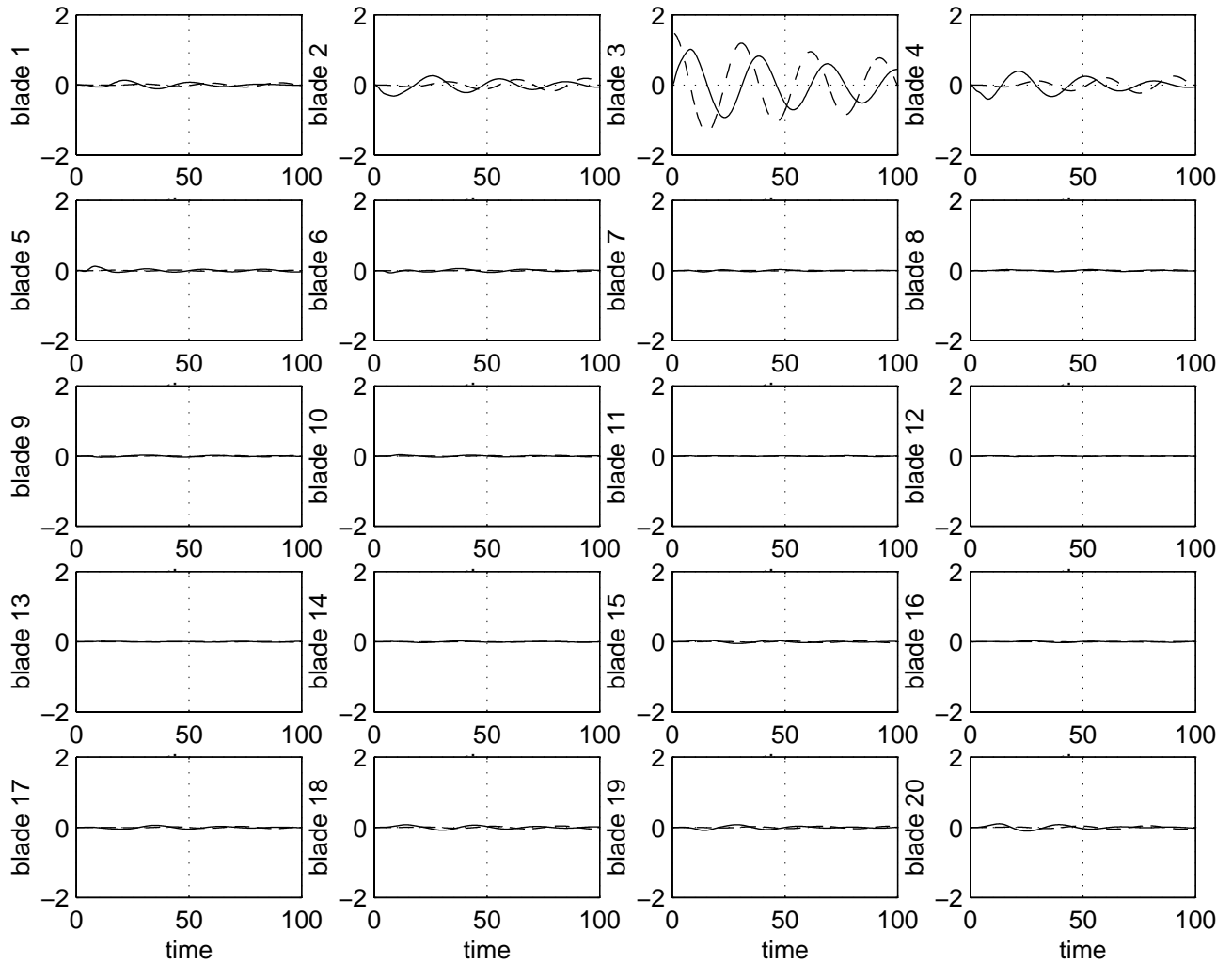


Figure 12: Coupled system response to an initial plunge displacement input at blade 3 : blade displacement (dashed line) and blade lift force (solid line).  $\mu = 100, k = 0.25, \zeta = 0$ .